Histopathological evaluation of the rabbit kidney after 10 and 30 days of subchronic peroral exposure to bendiocarbamate insecticide

Almasiova, V.[1], Holovska, K.[1], Cigankova, V.[1], Zyśk, B.[2]

[1] Department of Anatomy, Histology and Physiology, University of Veterinary Medicine and Pharmacy, Kosice, Slovak Republic

[2] Institute of Biology, Pedagogical University of Cracow, Podbrzezie 3, 31-054 Cracow, Poland

Introduction

In mammals, perorally applied carbamate pesticides are quickly absorbed into the bloodstream through the digestive system, and therefore distributed systemically. Inhibition of cholinesterase activity observed after bendiocarb administration is directly attributable to its insecticidal mode of action, i.e. reversible inhibition of acetylcholinesterase[3]. The inhibition of cholinesterase activity and the associated clinical signs are rapidly reversed upon cessation of exposure without long-term effect[4]. Due to high solubility of carbamates in lipids they easily pass across cytoplasmic membranes and rapidly reach various tissues (Marrs and Dewhurst, 2000). They are eliminated primarily with urine and excrements (Tós-Luty et al., 2001), so the kidneys and liver play a major role in their excretion. Although the neurotoxicity as the main impact of carbamates has been intensively studied (Alden et al., 1989; Debbarh et al., 2002; Kamboj et al., 2006), the influences on the kidney or liver have not been investigated in detail from the morphological point of view. Therefore the goal of this study was to elucidate the potential adverse effect of one of commonly used pesticide – bendiocarb, on structure and ultrastructure of kidneys after its peroral administration to adult rabbits at a dose of 5 mg/kg body weight per day. The kidney parenchyma was examined microscopically on days 10 and 30 of the experiment.

Materials and methods

The animals used in this study were divided to four groups, 10 animals per group. The animals from the control (C1) and first experimental (E1) group

[3] (http://www.pesticideinfo.org/Detail_Chemical.jsp?Rec_Id=PC32991).

[4] (http://www.who.int/whopes/quality/Bendiocarb_eval_WHO_jan_2009.pdf).

were euthanised on day 10, animals from the second control (C2) and second experimental (E2) group on day 30 of the experiment. Tissue samples of size up to 1 mm^3 were excised from five different regions of cortical as well as five different regions of medullary portion of the right kidney. The samples were fixed by immersion in 3% glutaraldehyde and postfixed in 1% osmium tetraoxide (both in 0.15 M cacodylate buffer, pH 7.2–7.4). After dehydration in acetone they were transferred to propylene oxide and embedded in Durcupan ACM. Ultrathin sections were cut using an ultramicrotome LKB Nova, double contrasted with uranyl acetate and lead citrate and examined under a Tesla BS 500 electron microscope. Semi-thin sections of specimens processed for transmission electron microscopy (TEM) were stained with toluidine blue and examined under a light microscope Jenamed.

Results

E1 group – light microscopy

After 10 days of the experiment the kidney parenchyma showed diffuse changes within the cortical (Fig. 1) as well as the medullary portion (Fig. 2) of kidney. While the kidney corpuscles were injured only sporadically, the nephron containing uriniferous tubules were affected systematically. The collecting tubules were mostly unchanged. The interstitium was characteristic in appearance (Fig. 1 and 2). The majority of kidney corpuscles revealed typical structure of glomerulus and double-layered Bowman's capsule consisting of podocytes and parietal layer. The urinary space was not enlarged. The intraglomerular mesangium was characteristic (Fig. 3).

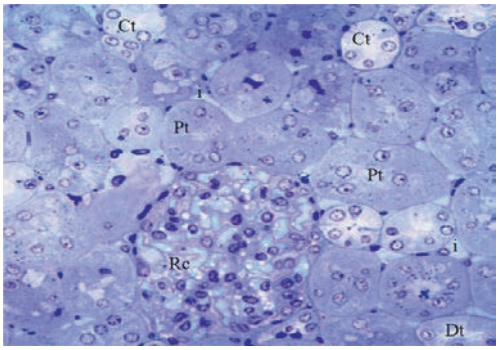

Fig. 1. Kidney cortex after 10-day exposure to bendiocarb (semi-thin section, toluidine blue), magnification 100×; Rc – renal corpuscle, Pt – proximal tubule, Dt – distal tubule, Ct – collecting tubule, i – interstitium

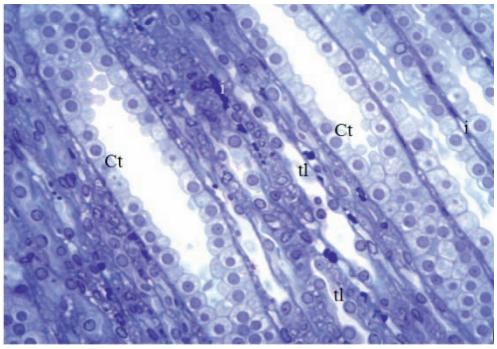

Fig. 2. Kidney medulla after 10-day exposure to bendiocarb (semi-thin section, toluidine blue), magnification 100×; Ct – collecting tubule, tl – thin limb of Henle's loop, i – interstitium

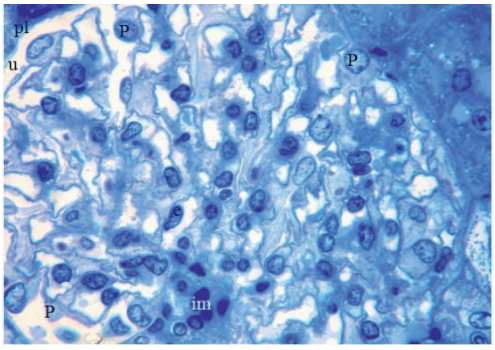

Fig. 3. Renal corpuscle with normal structure after 10-day exposure to bendiocarb (semi-thin section, toluidine blue), magnification 400×; e – endothelium of glomerulus, P – podocyte, pl – parietal layer of Bowman's capsule, u – urinary space, im – intraglomerular mesangial cells

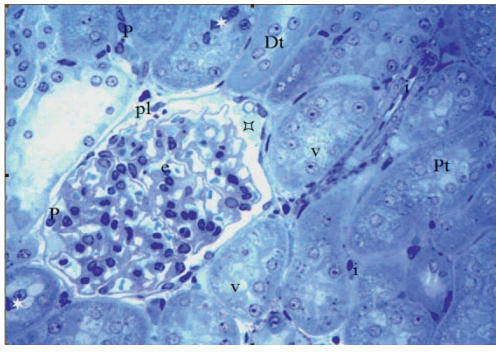

Fig. 4. Kidney cortex with slightly affected renal corpuscle and affected uriniferous tubules after 10-day exposure to bendiocarb (semi-thin section, toluidine blue), magnification 100×; ¤ – enlarged urinary space, e – endothelium of glomerulus, P – podocyte, pl – parietal layer of Bowman's capsule, Pt – proximal tubule, Dt – distal tubule, v – vacuoles, ✶ – necrotising cells, i – interstitium

The kidney cortex only rarely contained renal corpuscles with slightly enlarged urinary space, but the structure of the glomerulus and Bowman's capsule was typical (Fig. 4). Within the proximal tubules, every cell revealed cytoplasmic vacuolisation and shortening. Shortened cells within some proximal tubules were covered with incomplete and lower brush border. The distal tubules were lined with shorter cells and their lumina were subsequently more open. The cell cytoplasm was more vacuolated than in the controls. The collecting tubules had wide lumina and the cytoplasm of cells was pale. Cellular necrotisation and subsequent sloughing within the uriniferous and collecting tubules was seen only occasionally. A characteristic feature of the necrotising cells were shrunk and irregular nuclei. The interstitium was characteristic, without any apparent morphological changes (Fig. 4 and 5).

At a higher magnification, the vacuoles randomly distributed across the cytoplasm of proximal and distal tubules were more apparent. Nuclei of the cells inside proximal tubules were round and mitochondria typically abundant. These proximal tubules contained reduced and discontinuous brush borders. The cells lining the distal tubules were lower than in the controls. In sporadic cases, the tubules contained necrotising cells and lumina of uriniferous tubules contained sloughed material. The interstitium was typical in its extent and structure, and contained coherent blood vessels (Fig. 5). Kidney medulla contained collecting tubules with typical appearance, lined with typical cuboidal principal (light) and less numerous intercalated (dark) cells. The squamous cells lining the thin segments of Henle's loop were mostly regular. Interstitial components and blood vessels in the medullary region were normal (Fig. 6).

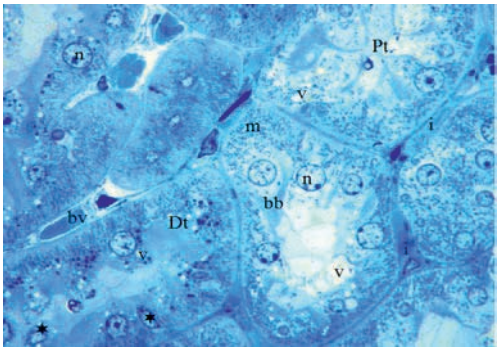

Fig. 5. Kidney cortex with affected uriniferous tubules after 10-day exposure to bendiocarb (semi-thin section, toluidine blue), magnification 400×; Pt – proximal tubule, Dt – distal tubule, v – vacuoles, n – nucleus, m – mitochondria, bb – brush border, ✶ – necrotizing cells, i – interstitium, bv – blood vessel

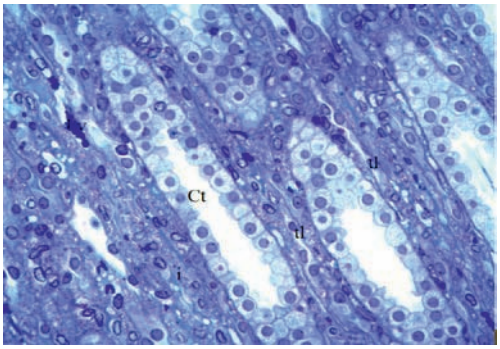

Fig. 6. Kidney medulla with normal collecting tubules and thin limbs of Henle's loop after 10-day exposure to bendiocarb (semi-thin section, toluidine blue), magnification 100×; Ct – collecting tubules, tl – thin limbs of Henle's loop, i – interstitium, bv – blood vessel

E2 group – light microscopy

There were more intensive diffuse changes within the cortical and medullary parenchyma of the kidneys after 30 days of the experiment. The kidney corpuscles were affected in two different ways. The first type of the renal corpuscles had enlarged urinary space as well as lumina of glomerular capillaries. The overall shape of podocytes and cells of the parietal layer of Bowman's capsule were often changed and their nuclei were mostly irregular. The intraglomerular mesangium appeared unchanged (Fig. 7). The second (and far less numerous) type of the renal corpuscles was totally disrupted. The size of these corpuscles was considerably reduced and their structure was very unusual. The cells of the parietal layer of Bowman's capsule and podocytes were damaged. The total shape of cells was irregular and nuclei were often deeply indented or even shrunk. The urinary space and lumina of glomerular capillaries were extremely wide and sometimes contained sloughed cells or cellular particles. The adjacent interstitium was enlarged and contained congested blood vessels (Fig. 8). The proximal tubules showed various morphological changes. The first type of tubules possessed wider and irregular lumina due to reduced height of the cells with additionally reduced brush borders.

Some epithelial cells were extremely low with only occasional microvilli instead of continuous brush border. Both cell types had typical round nuclei and higher number of vacuoles within the cytoplasm. The interstitium surrounding these tubules was enlarged and often infiltrated with blood elements as well as congested and incoherent blood vessels (Fig. 9).

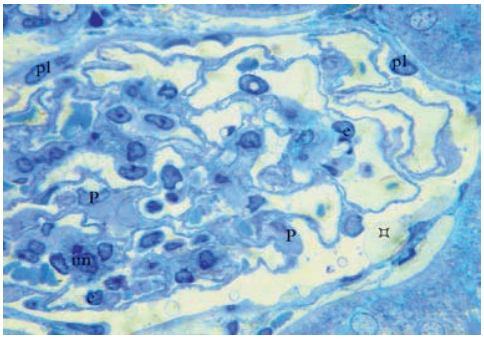

Fig. 7. The affected renal corpuscle after 30-day of exposure (semi-thin section, toluidine blue; TB), magnification 400×; e – endothelium of glomerulus, P – podocyte, pl – parietal layer of Bowman's capsule, ¤ – enlarged urinary space, im – intraglomerular mesangial cells

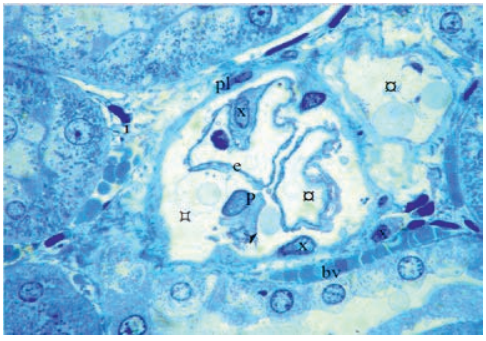

Fig. 8. Highly disrupted renal corpuscle after 30-day of exposure (semi-thin section, TB), magnification 400×; e – endothelium of glomerulus, P – podocyte, pl – parietal layer of Bowman's capsule, × – indented or shrunk nuclei, ¤ – enlarged urinary space, ¤ – wide capillary lumen, ⮟ – sloughed cells or cellular particles, i – interstitium, bv – blood vessel

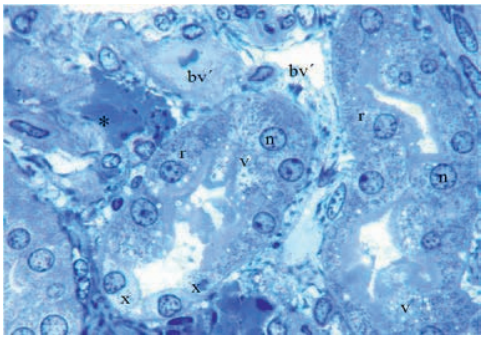

Fig. 9. The first type of affected proximal tubules and adjacent interstitium after 30-day of exposure (semi-thin section, TB), magnification 400×; r – epithelial cells reduced in height with reduced brush border, × – extremely low epithelial cells with only some microvilli, n – nucleus, v – vacuoles, * – infiltrations within the interstitium, bv´ – affected blood vessels

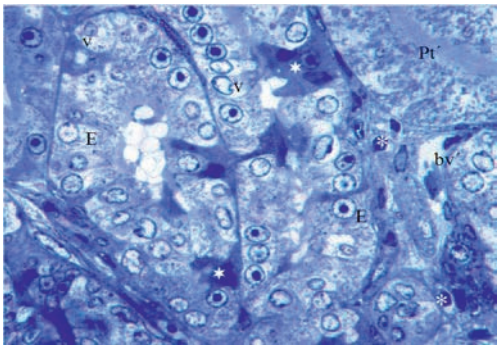

Fig. 10. Proximal tubules and adjacent interstitium with the second and third type of proximal tubules after 30-day of exposure (semi-thin section, TB), magnification 400×; E – relatively tall epithelial cells with reduced brush border, v – vacuoles, ✶ – necrotizing cells, Pt´ – relatively unaffected proximal tubule, * – infiltrations within the interstitium, bv´ – affected blood vessel

The second type of tubules was lined with relatively tall epithelial cells with vacuolated cytoplasm, regular nuclei and reduced brush border. There were numerous necrotizing cells randomly strewed among the above mentioned cells. The necrotizing cells were shrunk, dark and possessed dark and irregular nuclei. They were either solitary or formed small clumps (Fig. 10). Only rarely we observed the relatively characteristic proximal tubules (the third type) with complete and continuous brush borders. The wider interstitium contained a number of blood elements and congested blood vessels with broken walls (Fig. 10).

The distal tubules were lined with simple cuboidal epithelial cells with prominent protrusions due to the intense apical cytoplasmic vacuolization. The lumina of the distal tubules were consequently quite narrow. The nuclei of epithelial cells were round and regular and the basal regions of cells were rich in large and vertically-oriented mitochondria. Sloughed material was found inside the luminal space in some sections of distal tubules. The wider interstitium contained blood elements as well as affected blood vessels with irregular endothelium (Fig. 11). The cells of cortical and medullary collecting tubules were mostly typical in appearance, but their cytoplasm was more vacuolated than in the controls. Within some sections, the collecting tubules showed more intense cellular sloughing and their lumina contained clusters of sloughed material. The thin limbs of Henle's loop were lined with squamous cells highly irregular in shape. The interstitium was wider, more cellular and the blood vessels were lined with irregular endothelium (Fig. 12 and 13).

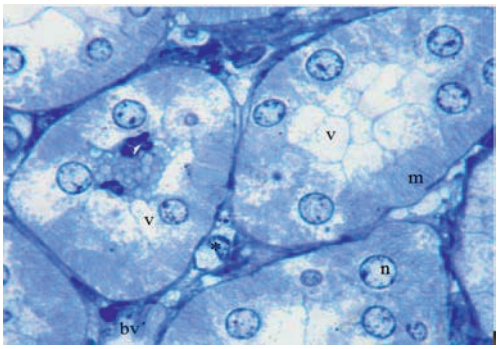

Fig. 11. Distal tubules lined with cells containing prominent apical vacuoles and adjacent interstitium after 30-day exposure to bendiocarb (semi-thin section, toluidine blue), magnification 1000×; v – apical vacuolisation, n – nucleus, m – mitochondria, ⩛ – sloughed material, * – infiltrations within the interstitium, bv´ – affected blood vessel

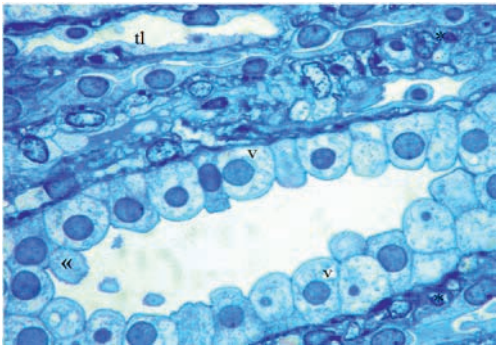

Fig. 12. Kidney medulla with a collecting tubule and thin limbs of Henle's loop after 30-day exposure to bendiocarb (semi-thin section, toluidine blue), magnification 1000×; v – vacuoles, « – sloughing cells, tl – thin limb of Henle's loop, * – infiltrations within the interstitium

E1 group – electron microscopy

Although the light microscopy failed to reveal some structural changes within the renal corpuscles, except for enlarged urinary spaces in some occasional renal corpuscles, the electron microscopy showed some ultrastructural differences in the majority of investigated podocytes. The first (and the most numerous) type of podocytes contained slightly more electronlucent cytoplasm with typical organelles. The pedicels of these podocytes were mostly characteristic in shape, but several pedicels were irregular. The primary processes, trabeculae, had typical shape and ultrastructure (Fig. 14).

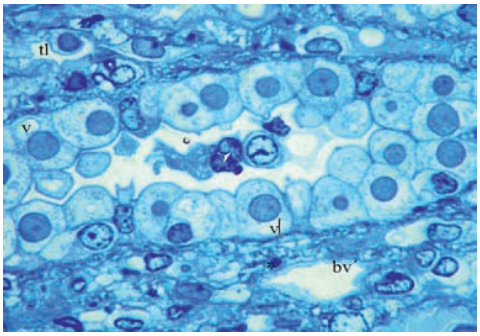

Fig. 13. Kidney medulla with a collecting tubule and thin limbs of Henle's loop after 30-day exposure to bendiocarb (semi-thin section, toluidine blue), magnification 1000×; v – vacuoles, ⩗ – sloughed material, tl – thin limb of Henle's loop, * – infiltrations within the interstitium, bv´ – affected blood vessel

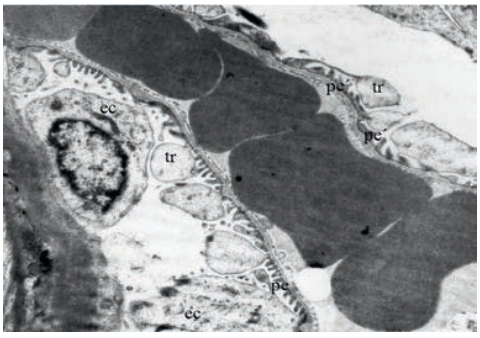

Fig. 14. The renal corpuscle containing podocyte with slightly more electronlucent cytoplasm, typical organelles and partly affected pedicles after 10-day of exposure (transmission electron micrograph), magnification 3200×; ec – slightly more electronlucent cytoplasm of the podocyte, tr – trabeculae, pe – regular pedicels, pe´ – irregular pedicels

Another (less numerous) type of podocytes had strong electronlucent cytoplasm, lacking the usual assortment of cellular organelles around the nucleus in comparison with the control counterpart. The pedicels of these podocytes were consistently irregular in shape and ultrastructure. Their cytoplasm contained a few microtubules and microfilaments. The glomerular basement membrane was habitually thick, noninterupted, and comprised three layers of different electron density, *lamina rara interna, lamina densa* and *lamina rara externa.* The fenestrated endothelium of glomerular capillaries was typical in appearance (Fig. 15).

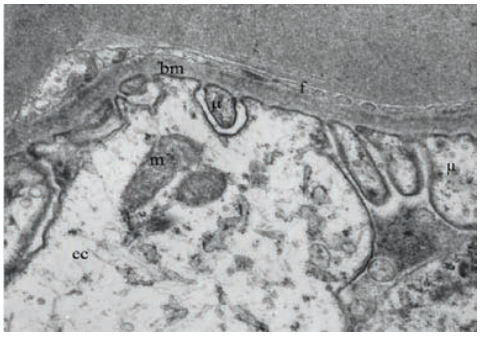

Fig. 15. Detail of the renal corpuscle in the area of the filtration slit barrier after 10-day exposure to bendiocarb (transmission electron micrograph), magnification 7400×; ec – more electronlucent cytoplasm of the podocyte body, μ – microfilaments and microtubules, bm – glomerular basement membrane, f – fenestrated endothelium

The main ultrastructural characteristic of cells within the proximal tubules was intense cytoplasmic vacuolisation. Vacuoles of different size, shape and density were distributed throughout the cytoplasmic content of cells. Other cellular organelles showed typical ultrastructure: the nuclei were round and regular and abundant elongated mitochondria occupied the basal portions of cells. The microvilli covering the apical surface of cells were shorter than usual and in some sections of proximal tubules also irregular (Fig. 16 and 17). The cells within the distal tubules possessed typical round nuclei and a number of typical vertically-oriented elongated mitochondria between the deep basal plasma membrane infoldings (Fig. 18).

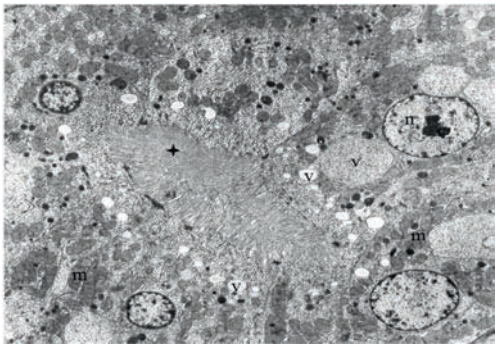

Fig. 16. The proximal tubule after 10-day exposure to bendiocarb (transmission electron micrograph), magnification 3200×; v – vacuoles, n – nucleus, m – mitochondria, ✦– shorter microvilli

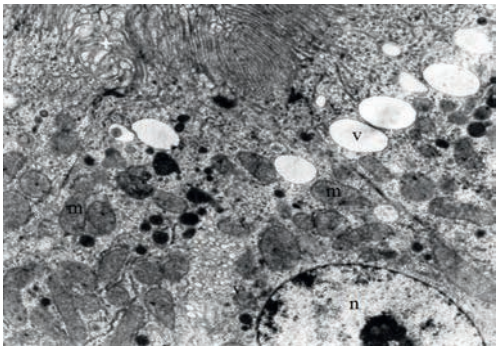

Fig. 17. Detail of the apical portion of proximal tubule with irregular microvilli after 10-day of exposure (transmission electron micrograph; TEM), magnification 9600×; v – vacuoles, n – nucleus, m – mitochondria, ✦ – irregular microvilli

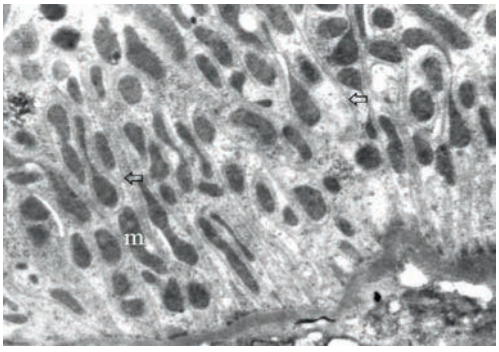

Fig. 18. Distal tubule with large and typically oriented mitochondria and deep plasma membrane infoldings after 10-day of exposure (TEM), magnification 6800×

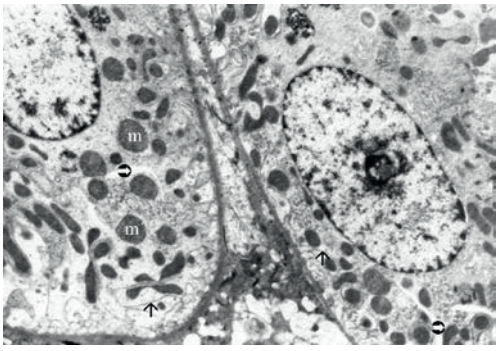

Fig. 19. Distal tubule with untypical and uncommonly oriented mitochondria and lateral intercellular disconnection after 10-day of exposure (TEM), magnification 5200×; m´ – changed mitochondria, ↑ – shallow plasma membrane infoldings, ➲ – intercellular disconnection

Only occasional sections of the distal tubules contained cells with large mitochondria of untypical shape and orientation and plasma membrane formed only shallow basal infoldings. Some cells were detached from one another within such type of tubules (Fig. 19).

Although the structure of cortical and medullary collecting tubules appeared to be normal under the light microscope, the electron microscopy revealed higher number of cytoplasmic vacuoles in some tubular sections. The nuclei were round and typical and the mitochondria were randomly scattered throughout the cytoplasm (Fig. 20).

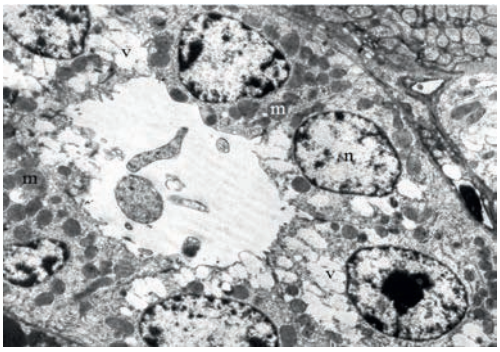

Fig. 20. Collecting tubule with cellular vacuolisation after 10-day of exposure (TEM), magnification 3200×; v – vacuoles, n – nucleus, m – mitochondria

The ultrastructure of thin limbs of the Henle's loop was mostly characteristic. Squamous cells possessed typical oval nuclei, mitochondria with normal ultrastructure, and the apical side of cells was covered by several short microvilli. The vacuoles were infrequent. Rarely, in some segments, cells lost their lateral intercellular connection between each other (Fig. 21).

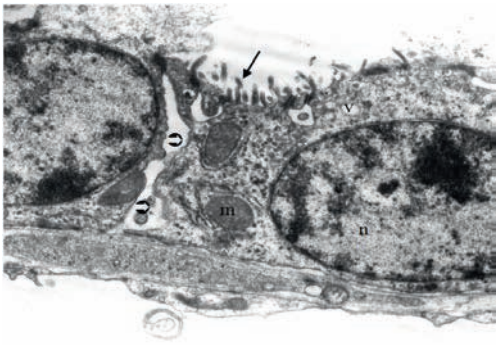

Fig. 21. Disrupted intercellular connection within the Henle's loop segment after 10-day of exposure (TEM), magnification 9600×; ➲ – disconnection, n – nucleus, m – mitochondria, ➞ – microvilli, v – vacuoles

E2 group – electron microscopy

Electron microscopy showed more substantial ultrastructural changes within components of the nephron and collecting tubules after 30 days of the experiment. Structural components of all investigated renal corpuscles were affected. The cytoplasm of podocytes was more electrondense in comparison with the controls and contained swollen mitochondria. The nuclei of podocytes were oval-shaped. The podocyte projections, trabeculae and pedicels, were irregular and their surface was often not smooth, but rather rough and smudgy. The thickness of basement membrane delimiting the podocytes and fenestrated glomerular capillaries was uneven. The fenestrated endothelium was mostly irregular in shape (Fig. 22). The proximal tubules were lined with shorter cells with reduced and irregular microvilli. The cytoplasm of cells contained many vacuoles and the ultrastructure of cellular organelles was relatively characteristic. Some cells possessed swolen mitochondria. Several sections of proximal tubules contained increased quantity of necrotising cells with extremely electrondense cytoplasm, shrunk nucleus, swollen mitochondria and a number of electronlucent vacuoles (Fig. 23). The cells within the distal tubules possessed round nuclei, numerous mitochondria and large apical vacuoles of varying electrondensity. Several cells had swollen mitochondria, and in some sections the cells were disconnected (Fig. 24 and 25). Some tubules contained individual necrotising cells with highly disorganised and electrondense cytoplasm (Fig. 26). The cells of the collecting tubules had typical round nuclei and their cytoplasm contained normal or swollen mitochondria and numerous, randomly distributed electronlucent vacuoles (Fig. 27). The thin limbs of the Henle's loops had clearly detached squamous epithelial cells. Their nuclei were mostly regular round, and their cytoplasm contained characteristic mitochondria. The apical surface of cells was covered with several short microvilli. Some cells were more elongated (Fig. 28).

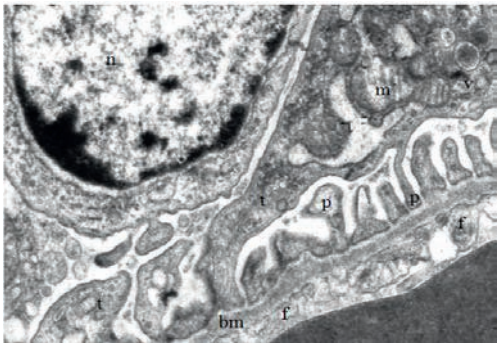

Fig. 22. Part of the renal corpuscle with considerably changed ultrastructure after 30-day exposure to bendiocarb (transmission electron micrograph), magnification 9800×; n – nucleus, m´ – swollen mitochondria, t – trabecula, p – pedicel, bm – basement membrane, f – fenestrated glomerular endothelium

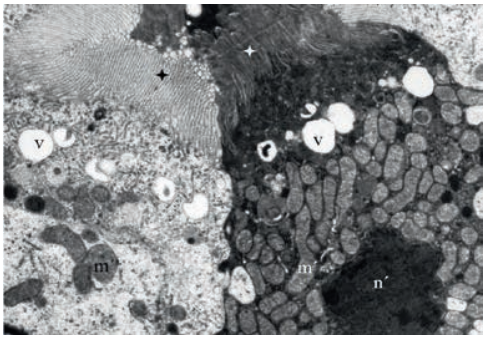

Fig. 23. Detail of the normal and necrotising cell within the proximal tubule after 30-day exposure to bendiocarb (transmission electron micrograph), magnification 7300×; n´ – shrunk nucleus, m´ – swollen mitochondria, v – vacuoles, ✦ – microvilli

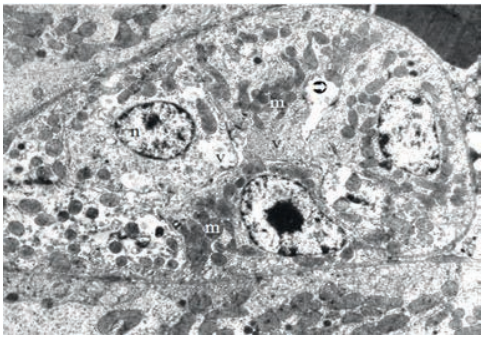

Fig. 24. Distal tubule with the disconnected cells after 30-day exposure to bendiocarb (transmission electron micrograph), magnification 3200×; n – nucleus, m – swollen mitochondria, v – vacuoles, ➲ – disconnected cells

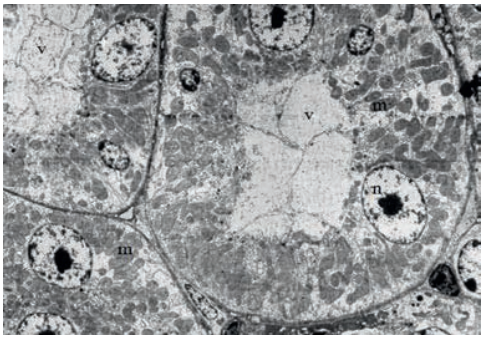

Fig. 25. Distal tubule with large apical vacuoles after 30-day exposure to bendiocarb (transmission electron micrograph), magnification 3200×; n – nucleus, m – normal mitochondria, v – vacuoles

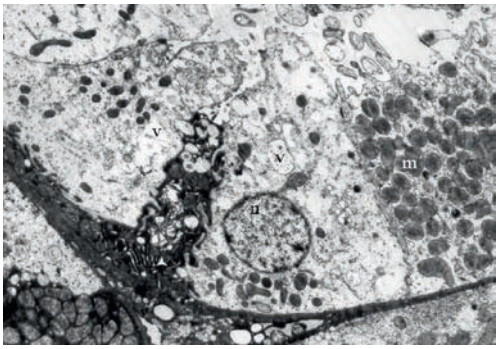

Fig. 26. Distal tubule with the necrotising cell after 30-day exposure to bendiocarb (transmission electron micrograph), magnification 3200×; n – nucleus, m´ – swollen mitochondria, v – vacuoles, ⅄ – necrotising cell

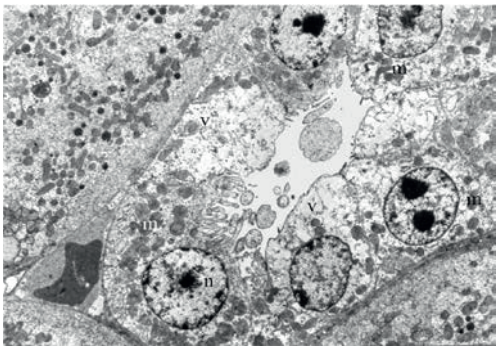

Fig. 27. Collecting tubule with highly vacuolated cytoplasm after 30-day exposure to bendiocarb (transmission electron micrograph), magnification 3200×; n – nucleus, m – normal mitochondria, m´ – swollen mitochondria, v – vacuoles

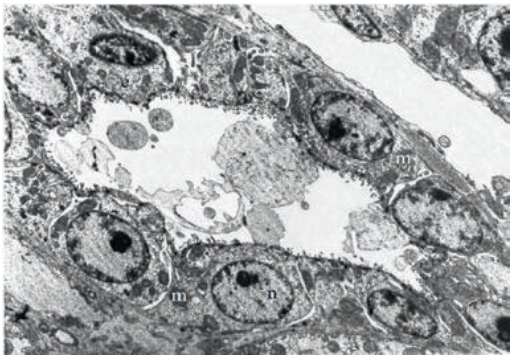

Fig. 28. Loop of Henle with clearly detached squamous epithelial cells after 30-day exposure to bendiocarb (transmission electron micrograph), magnification 3200×; n – nucleus, m – mitochondria, e – more elongated epithelial cells

Discussion

In vertebrates, the carbamates are subjected to hydrolysis and hydroxylation by the liver enzymes (Mac Pherson et al., 1991) which results in formation of metabolites, such as the conjugated glucuronides and sulphates (Chen and Dorough, 1979). For example, the primary metabolite in rat urine is the conjugated phenol, 2,2-dimethyl-1, 3-benzoxodiol-4-ol (Chalis and Adcock, 1981). Carbamate pesticides do not accumulate in mammalian tissues[5] but are rapidly, up to 48 hours excreted in the form of metabolites or in unchanged form, primarily by urine – about 90%, faeces and expired air – about 10% (Tós-Luty et al., 2001). This suggests increased load on the excretory organs, particularly on kidneys.

The present study clearly proved an adverse effect of bendiocarbamate insecticide Bendiocarb on the structure and ultrastructure of kidneys in experimental rabbits after 10 and particularly 30 days of oral administration. We observed diffuse changes of varying intensity in cortical and medullary portion of kidney parenchyma.

Although after 10 days of the experiment the sites of the blood filtration, the kidney corpuscles, were only ocassionally altered, after 30 days each kidney corpuscle showed signs of moderate to strong degeneration. The renal corpuscles had enlarged their urinary spaces, and two-layered Bowman's capsule as well as glomerulus were structurally changed. Similar ultrastructural changes within the kidney corpuscles were noted in rats after prolonged administration of low doses of mancozeb (subclass of carbamate pesticide called dithiocarbamate) the kidney corpuscles of which showed degenerated endothelium of the glomerular capillaries, basal lamina and podocytes (Salem, 2011). Wide urinary space and mesangial hypercellularity (Morsy, 2003) or degeneration of Bowman's capsule and rudimentary glomerulus (Kumar et al., 2011) were found in kidneys of rats after peroral administration of organophosphates, which, similar to carbamates, express their toxicity to attack the nervous system by inhibiting cholinesterase. Caglar et al. (2003) in ultrastructural evaluation of the effect of organochlorine insecticide also described glomerular alterations, such as the fusion of podocyte pedicels and focal thickening at glomerular basal membrane in some kidney corpuscles. Glomerular degeneration and occasional atrophy, both observed in the present study, was described in mice after metalaxyl fungicide administration (Sakr et al., 2011). All above described histopatological changes are closely consistent with the present study. Such structural and ultrastructural changes may cause increased filtration of high molecules (e.g. plasma proteins) with consecutive proteinuria (Choi et al., 2010; Gagliardini, 2010) or, on the other hand, diminishing ability to filter creatinine with subsequent serum creatinine rises (Capcarova et al., 2010).

[5] (http://www.inchem.org/documents/jmpr/jmpmono/v82pr05.htm).

The proximal tubules which reabsorb the necessary material and secrete ions (including toxins) are supposed to be highly loaded nephron components. The present findings exactly confirmed this concept because they were constantly affected during both experimental periods. After 10 days of the experiment the cells within the proximal tubules were generally lower and their brush borders were reduced. The cytoplasm contained increased number of pale vacuoles which clearly demonstrated elevated transepithelial transport. The proximal tubules were more seriously affected after 30 days of the experiment. They were generally lined with shorter cells with reduced brush borders and their cytoplasm contained a number of vacuoles. These tubules also contained extremely shortened cells without brush borders. Some tubules were lined with relatively high epithelial cells with vacuolated cytoplasm, regular nuclei and reduced brush border. The cytoplasmic content of the above described cells was mostly characteristic, however, several investigated cells contained swollen mitochondria. Similar signs of tubulonephrosis after using different dithiocarbamate or organophosphate formulations were noted in rats after subchronic peroral administration (Salem, 2011; Tós-Luty et al., 2001). The prominent mitochondrial degeneration in proximal convoluted tubules was also evident in mice kidneys after endosulfan administration (Caglar et al., 2003). The exfoliation of tubular epithelium and signs of the cellular necrotization, such as the pyknotic nuclei, in addition to intensive cytoplasmic vacuolization were noticed by many authors (Sakr et al., 2011; Lin and Garry, 2011; Debbarh et al., 2002). The severe signs observed in the present study indicate that carbamates probably boost cellular necrotisation.

The distal tubule, also referred to as diluting segment due to sodium, chloride and calcium reabsorbtion, also showed structural changes. After 10 days of the experiment, the epithelial cells were reduced in size and the cytoplasm contained higher number of small vacuoles distributed throughout the cytoplasm. Occasional tubules possessed sloughed material within the lumen. After 30 days of the experiment, the apical portions of cells formed extremely prominent protrusions toward the lumen due to strong cytoplasmic vacuolisation and the cells were generally rich in mitochondria. Several cells had swollen mitochondria and others were detached. The specific cytoplasmic protrusions as well as cellular detachment may suggest defects in the cytoskeleton of cells (Caglar, 2003). Necrotisation within the distal tubules was not as intense as in proximal tubules. Similar vacuolar degeneration and focal area of necrosis were also observed by many authors after organophosphate or organochlorine treatment (Salem, 2011; Alden et al., 1989; Torki et al., 2001; Morsy, 2003; Caglar, 2003).

The collecting tubules did not show any histopathological changes after 10 days of the experiment but after 30 days the cytoplasm of cells contained vacuoles which may suggest intensification of the acid-base balance regulation. Some sections of medullary collecting tubules revealed more intense cellular sloughing.

The thin limbs of Henle's loop were lined with typical cells after 10 days of the experiment, but after 30 days they were highly irregular in shape.

However, after 10 days of exposure the interstitium did not reveal signs of hypercellularity, but after 30 days it was wider, more cellular and the blood vessels were often affected.

All in all, the degenerative changes across the nephron components and collecting tubules confirmed the subchronic toxic effect of bendiocarb or its metabolites on cells, involving most likely the oxidation of lipid membranes. The reactive oxygen species most probably play a role in changing configuration of plasma membranes and seem to account for the structural and ultrastructural alteration of kidneys or other tissues (Gupta et al., 2007; Kamboj et al., 2006; Kumar et al., 2011; Marnett, 1997). Therefore exploitation of the protective effect of various antioxidants, such as curcurmin (Kumar et al., 2011), ginger (Sakr et al., 2011), vitamin C and ginseng (Morsy, 2003), against the negative effect of various pesticides, together with recommended usage of pesticides particularly in agriculture, may appear very helpful.

Conclusions

Generally the kidney parenchyma was clearly defective in structure and ultrastructure after peroral exposure to bendiocarb administered at a dose of 5 mg/kg per day during 10 and 30 experimental days. The changes within various nephron components, collecting tubules and interstitium were more intense after 30 days of the experiment. The kidney corpuscles, proximal and distal tubules, thin limbs of the loop of Henle and collecting tubules showed signs of clear degeneration of varying intensity. Considerable cellular necrotisation was observed especially within the proximal tubules. The above mentioned morphological changes signify impaired function of the kidneys at the level of filtration, resorption or secretion.

References

Alden, C.I., Parker, R.D., Eastman, D.F. (1989): Development of an acute model for the study of chloromethane diphosphonate nephrotoxicity. Toxicol. Pathol., 17, 27–32.

Caglar, Y., Kaya, M., Belge, E., Mete, U.O. (2003): Ultrastructural evaluation of the effect of endosulfan on mice kidney. Histol. Histopathol., 18, 703–708.

Capcarova, M., Petrovova, E., Flesarova, S., Dankova, M., Massanyi, P., Danko, J. (2010): Bendiocarbamate induced alterations in selected parameters of rabbit homeostasis after experimental peroral administration. Pestic. Bioch. Physiol., 98, 213–218.

Debbarh, I., Rambelomanana, S., Penouil, F., Castaigne, F., Poisot, D., Moore, N. (2002): Human neurotoxicity of ethylene-bis-dithiocarbamates (EBCD). Rev. Neurol., 158, 1175–1180.

Gagliardini, E., Conti, S., Benigni, A., Remuzzi, G., Remuzzi, A. (2010): Imaging of the porous ultrastructure of the glomerular epithelial filtration slit. J. Am. Soc. Nephrol. Dec., 21, 2081–2089.

Gupta, R.C., Milatovic, S., Dettbarn, W.D., Aschner, M., Milatovic, D. (2007): Neuronal oxidative injury and dendritic damage induced by carbofuran: protection by memantine. Toxicol. Appl. Pharmacol., 219, 97–105.

Challis, I.R., Adcock, J.W. (1981): The Metabolism of the Carbamate Insecticide Bendiocarb in the Rat and in Man. Pestic. Sci., 12, 638–644.

Chen, K.C., Dorough, H.W. (1979): Glutathione and mercapturic acid conjugations in the metabolism of naphtalene and 1-naphtyl N-methylcarbamate (carbaryl). Drug. Chem. Toxicol., 2, 331–354.

Choi, S.Y., Suh K.S., Choi, D.E., Lim, B.J. (2010): Morphometric analysis of podocyte foot process effacement in IgA nephropathy and its association with proteinuria. Ultrastruct. Pathol., 34, 195–198.

Kamboj, A., Kiran, R., Sandhir, R. (2006): Carbofuran-induced neurochemical and neurobehavioral alterations in rats: attenuation by N-acetylcysteine. Exp. Brain Res., 170, 567–575.

Kumar, R., Kumar, A., Singh, J.K., Nath, A., Ali, M. (2011): Study of bioremedial impact of Cucurmin on Chloropyrifos induced kidney damage in mice. Pharm. Glob., 2.

Lin, N., Garry, V.F. (2011): *In vitro* studies of cellular and molecular developmental toxicity of adjuvants, herbicides, and fungicides commonly used in Red River Valley, Minnesota. J. Toxicol. Environ. Health. A., 60, 423–439.

Mac Pherson, S.E., Scott, R.C., Williams, F.M. (1991): Fate of carbaryl in rat skin. Arch. Toxicol., 65, 594–598.

Marnett, L.J. (1997): Lipid peroxidation – DNA damage by malondialdehyde. Mutation Res., 424, 83–95.

Marrs, T.C., Dewhurst, I.: Toxicology of pesticides. General and Applied Toxicology. Lavoisier S.A.S.: London-New York; 2000, 1993–2012.

Morsy, F.A. (2003): Protective effect of vitamin C and Ginseng on experimental liver and kidney injuries induced by insecticide prophenophos in male rats. The Egypt. J. of Hosp. Med., 10, 34–51.

Sakr, S.A., Lamfon, H.A., Essawy, A.E. (2011): Ginger (*Zingiber officinale*) extract ameliorates metalaxyl fungicide induced nephrotoxicity in albino mice. Afr. J. Pharm. Pharmacol., 5, 104–112.

Salem, M.M. (2011): Toxic effects of mancozeb containing formulations and neemix pesticides on kidney function and ultrastructure of albino rats. Acad. J. Biolog. Sci., 3, 17–30.

Torki, M.A., Elrahman, A., Sobhy, H.M., Mohamed, I.E. (2001): Comparative study of the toxic effect of the organophosphorus insecticide (Prophenophos) and microbial pesticide (Biofly) on rats. J. Egypt. Soc. Toxicol., 24, 29–36.

Tós-Lúty, S., Przebirowska, D., Latuszynska, J., Tokarska-Rodak, M. (2001): Histological and ultrastructural studies of rats exposed to carbaryl. Ann. Agric. Environ. Med., 8, 137–144.

http://www.inchem.org/documents/jmpr/jmpmono/v82pr05.htm (accessed Oct. 2001).

http://www.pesticideinfo.org/Detail_Chemical.jsp?Rec_Id=PC32991

http://www.who.int/whopes/quality/Bendiocarb_eval_WHO_jan_2009.pdf